DFT-guided Development of New Hemilabile (P^N) Ligands for Gold-(I/III) RedOx Catalysis : Application to the Thiotosylation of Aryl Iodides

Karim Muratov, Emil Zaripov, Maxim V. Berezovski and Fabien Gagosz*

Department of Chemistry and Biomolecular Sciences, University of Ottawa, Ottawa, K1N 6N5 (Canada)

ABSTRACT: Ligand-enabled oxidative addition of Csp^2-X bonds to Au(I) centers has recently appeared as a valuable strategy for the development of catalytic RedOx processes. Several cross-coupling reactions that were previously considered difficult to achieve were reported lately, thus expanding the synthetic potential of gold(I) complexes beyond the traditional nucleophilic functionalization of π-systems. MeDalPhos has played an important role in this development and, despite several studies on alternative structures, remains so far, the only general ligand for such process. We report herein the discovery and the DFT-guided structural optimization of a new family of hemilabile (P^N) ligands that can promote oxidative addition of aryl iodides to gold(I). These flexible ligands, which possess a common 2-methylamino heteroaromatic *N*-donor motif, are structurally and electronically tunable, beyond being easily accessible and affordable. The corresponding Au(I) complexes were shown to outperform the reactivity of (MeDalPhos)Au(I) in a series of alkoxy- and amidoarylation of alkenes. Their synthetic potential and comparatively higher reactivity were further highlighted in the thiotosylation of aryl iodides, a challenging unreported C-S cross-coupling reaction that could not be achieved under classical Pd(0/II) catalysis and that allows a general and divergent access to aryl sulfur derivatives.

INTRODUCTION During the last two decades, homogeneous gold catalysis has evolved into becoming a powerful synthetic tool for the generation of structural diversity and molecular complexity, with applications in various fields including natural products and small bioactive molecules synthesis, material and biomolecular sciences.[1] This strong and sustained development has been fueled, for its great part, by the electrophilic properties of cationic gold species which have revealed to be exceptionally active towards the functionalization of carbon p systems by a variety of nucleophiles. In sharp contrast with the reactivity of commonly employed transition metals such as Pd or Ni,[2] Au-mediated RedOx catalysis, and more especially the development of cross coupling reactions, has been very limited.[3] This situation is mainly related to the comparatively high Au(I/III) RedOx potential (E_{red}° $Au^{(III/I)}$ = 1.41 V). As a result, most of the initially developed catalytic processes involved the use of a strong sacrificial oxidant to allow the difficult conversion of a linear (organo)gold(I) intermediate **1** into a square planar Au(III) complex **2** (Figure 1-A).[3e,4] Aryldiazonium salts **3** and photoredox catalysis were later found to be a useful combination to functionalize aryl moiety *via* the generation of structurally similar Au(III) complexes **4** (Figure 1-A).[3f,3m,5] However, the use of strong oxidants and diazonium salts inherently limits the synthetic potential of such approaches. A ligand strategy was found particularly appropriate to alleviate these constraints and provide new avenues for the oxidative addition of C-X bonds to Au(I) centers. The use of bidentate ligands that can confer stability to the resulting Au(III) complex (**5**→**6**, Figure 1-A), was key to further developments in the field of gold RedOx catalysis.[3a-d] Main bidentate ligands currently known to promote oxidative addition are represented in Figure 1-B.[6] Complex **12** featuring the small bite angle bidentate (P^P) ligand **7** (DPCb) was a breakthrough discovery made by Bourissou and coworkers in 2014.[7] No catalytic transformation was however developed with **7**. The hemilabile MeDalPhos (P^N) ligand (**8**) was introduced in the field by the same group three years later.[8] The corresponding (MeDalPhos)AuCl complex **13** was found to possess a remarkable reactivity that has been exploited over the past 6 years in the development of catalytic processes allowing C-C, C-N, C-O and C-S bond formation by cross-coupling with aryl iodides.[8,9] Bower and Russel reported that the use of simple (N^N) bidentate Bpy ligand (see **9**) could also favor oxidative addition to Au(I) but the corresponding Au(III) complexes were found too fragile for catalysis.[10] Very recently, the interest has been focusing onto the development of catalysts bearing (C^N) ligands. The same authors, and Zhang and Szostak, independently reported that the ImPy carbene-based ligand **11** represented a promising alternative to the use of MeDalPhos.[11] The related (MIC^N)AuCl complex **10** developed by the group of Ribas appeared to be less reactive.[12] Notably, oxidative addition energy barriers with (C^N) ligand **11** have been calculated to be significantly higher than when MeDalPhos is employed, what may represent some potential limitation for further development.[11b] While it is now well established that the strategy of using bidentate ligands to enable oxidative addition of C-X bonds to Au(I) centers is effective, it remains that the number of available ligands allowing catalytic processes is extremely limited. (MeDalPhos)AuCl (**13**) remains the only general precatalyst and therefore the go-to when developing a new RedOx transformation.[9]Surprisingly, very limited work has been done with respect to modifying the structure of MeDalPhos, which, in fact, is a repurposed ligand not initially designed for Au catalysis.[13]

Figure 1. Approaches in Au(I/III) RedOx catalysis, ligands enabling oxidative addition of C-X bonds to Au(I) centers and our strategy for the development of new (P^N) ligands.

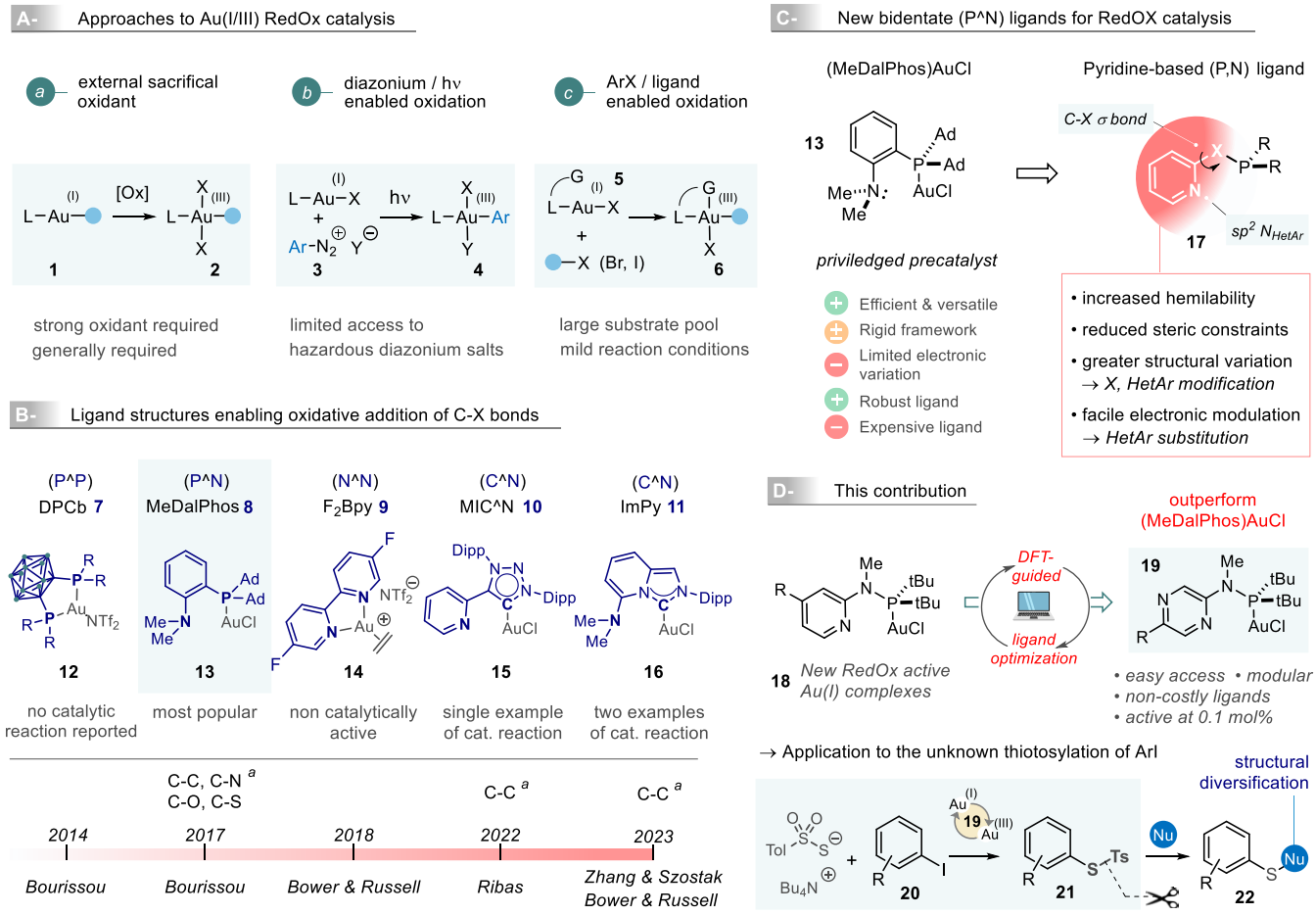

[a] Nature of the bond produced by Au-catalyzed cross-coupling reaction.

In the context of a C-N and C-C cross-coupling reactions, Patil and coworkers evaluated several alterations of the MeDalPhos structure, namely substitution at the N and P atoms, but none of the DalPhos analogs tested were found competitive.[9b,g] The group of Nevado also described the synthesis of Au(III) oxidative addition complexes supported by bidentate ligands analogous to MeDalPhos, but no catalytic transformation was reported.[14] Despite being a privileged ligand, MeDalPhos possesses a very rigid and compact structure with limited possibility to efficiently tune the electronics (Figure 1-C). This is more especially true for the N-donor atom given the orthogonality between the lone pair of electrons and the aromatic p system, what would likely limit the effect of aromatic substitution. According to the study on C-N cross-coupling reactions by Patil,[9b] electron rich and sterically demanding adamantyl groups on the P atom are also primordial for the catalytic activity. Their replacement by either Cy or Ph groups led to a ≈ 50% and ≈ 75% reduced catalytic efficiency, respectively. The same modifications even led to a complete loss of activity in their study on the alkoxyarylation of alkenes.[9h] In this context, we considered developing new (P^N) ligands that would allow more structural variation and an easier modulation of their electronics. Our strategy, described in Figure 1-C, relies on the replacement of the dimethylaniline moiety by a pyridine N-donor[12,15] that would be linked to the phosphanyl moiety by a one-atom X tether (see **17**). As such the possibility to produce a 5-membered chelate would be retained. Compared to MeDalPhos, such a ligand would be less rigid. Its hemilability would be increased thanks to the introduction of the C-X σ-bond, and the inclusion of the N-atom donor in the heteroaromatic ring would reduce the steric constraints around the metal center. More importantly, the structural changes would allow a facile modulation of the ligand electronics by direct substitution at the pyridine ring or by modification of the X tether.

We report herein the results of our investigations (Figure 1D) which have led to the development of a new family of (P^N) ligand for Au(I/III) RedOx catalysis. A DFT-guided

optimization of the initially designed ligands **18** allowed for the discovery of highly efficient catalysts **19** whose activity surpasses that of the (MeDalPhos)Au(I) standard for a series of alkoxy- and amidoarylation of alkenes. To further demonstrate the potential of these new catalysts, a gold-catalyzed thiotosylation of aryl iodides (**20**→**21**) was developed that allows a general and divergent access to arylsulfur derivatives **22**. Strikingly, this unknown cross-coupling could not be achieved via Pd(0/II) catalysis. The work was concluded by a computational and experimental study supporting the key role played by silver salts in this challenging catalytic C-S cross coupling.

RESULTS AND DISCUSSION

Synthesis, analysis, and reactivity of pyridine-based (P^N) Au(I) complexes. We started our investigations with the synthesis of the targeted bidendate (P^N) ligands and the corresponding AuCl complexes. Our methodology is presented in Figure 2-A. Among the various structural variations that could be considered, N and O linkers between the pyridine core and the phosphanyl moiety were selected since they would be easy to install from readily available starting materials (2-hydroxy/amino pyridines **23** & chlorophosphines **24**). This choice was made despite the potential lability of resulting P-O and P-N bonds but expecting the accessibility to the P center to be reduced in the metallic complexes **25.**16 Position C(4) of the pyridine was considered for substitution as it would allow a modulation of its electronics (and consequently its interaction with the Au center) without introducing steric constraints. The expensive Ad_2P fragment found in MeDalPhos was disregarded,[17] and the more accessible and convenient to introduce P*t*Bu_2, PCy_2 and PPh_2 groups selected for evaluation. To assess the potential ability of the corresponding (P^N) AuCl complexes **25** to be used as catalysts in RedOx processes, a set of two stoichiometric experiments were employed: the oxidative addition of **25** into the C-I bond of *p*F-iodobenzene to produce aryl-Au(III) complex **26** (Exp1),[8] and the oxidation of **25** into the Au(III)Cl_2 complex **27** by treatment with $PhICl_2$ (Exp 2).[12b,18] These reactions could be easily monitored and/or analyzed using ^{31}P, ^{19}F and ^{1}H NMR spectroscopy. Among the series of pyridine-based (P^N) AuCl complexes that were synthesized and tested (8),[19,20] we were very pleased to discover that complexes **28** possessing the MeN-PtBu_2 subunit could be converted into the corresponding Au(III) complexes **29** and **30** in a very efficient manner (Figure 2-B). The presence of this structural motif was found crucial. Exchanging the NMe fragment for a simple O atom or replacing the Me group by a H or a longer *n*Bu alkyl chain led to a complete loss of reactivity or to a very unselective reaction (*n*Bu).[20] Similarly, no activity was observed when the P*t*Bu_2 group was altered. From a synthetic point of view, the three AuCl complexes **28**$_{H,OMe,CF3}$ were easily obtained in a 2-step sequence starting from the corresponding 2-NMe pyridine **30** (Figure 2-C). This route is not only rapid but, amenable to gram scale synthesis and rather cheap. It also allows for a rapid structural diversification since 2-NMe pyridines **30** are either commercially available or easily accessible from < $2/g building blocks.[21] The potential lability of the ligand P-N bond was evaluated by studying the stability of the AuCl complex **28**$_H$ in MeOH. No decomposition was observed by ^{31}P NMR spectroscopy analysis after 2 weeks at 20 °C and only 10% of degradation could be detected after 7 days at 60 °C, thus demonstrating the robustness of the ligand structure.[20] As for the oxidative addition reaction with 4-F-iodobenzene, isolated yields ranging from 82 to 97% were obtained (Figure 2-B). Complexes **29**$_{H,OMe,CF3}$ were formed and isolated as chloride derivatives, which is the likely result of a thermodynamically driven salt metathesis event between the AgCl by-product and the initially produced iodo-Au(III) oxidative addition complex. Similar observations were previously made using either MeDalPhos, a biPy or a NHC ligand.[8,10b,11b] Complexes **29**$_{H,OMe,CF3}$ were found very stable at room temperature, easy to handle and manipulate. Comparatively, Au(III)Cl_2 complexes **30**$_{H,OMe,CF3}$ appeared to be more sensitive and were obtained in moderate to excellent yields (49-94%). The use of the NTf_2^- counteranion was required to prevent their degradation and make their isolation possible.[22] The structural changes induced by the oxidative processes on the (P^N)Au subunit could be directly observed by NMR spectroscopy analysis. As seen in Figure 2-D for the oxidation of Au(I) complex **28**$_H$ into the (P^N) Au(III) complexes **29**$_H$ and **30**$_H$, the ^{1}H chemical shifts of the pyridine hydrogen atoms increase upon oxidation at the Au center as the result of the coordination of the N_{pyr} atom to gold. As it could be expected, the effect was far more pronounced for the *ortho* and *para* positions to N, the $\Delta\delta$ of the H_{ortho} being approximately twice that of H_{para}. The $\Delta\delta$ was also more significant for the formation of **30**$_H$ ($\Delta\delta_{Hortho}$= 1.43 ppm) than for that of **29**$_H$ ($\Delta\delta_{Hortho}$= 1.16 ppm) most probably due to the higher electropositivity of the Au center in **30**$_H$. Notably, this variation in chemical shift was dependent on the nature of the substituent at position C(4) of the pyridine, with a maximum of $\Delta\delta_{Hortho}$= 1.55 ppm reached with the formation of **30**$_{CF3}$. The ^{31}P NMR chemical shifts were also affected by the oxidation of the gold center. The signal observed for the $Au^{(I)}$ complex **28**$_H$ at δ= 125.3 ppm raises up to δ= 156.4 ppm for $Au^{(III)}$ complex **30**$_H$.[23] The structures of Au(III) complexes **29**$_H$ and **30**$_H$ were confirmed by SCXRD analysis showing a slightly distorted square planar environment around the Au center, and an aryl moiety positioned *trans* to the N atom. Selected measurements are given in Figure 2-D. The structures were found similar to those previously reported with the MeDalPhos ligand.[12b,14]

Figure 2. Synthesis of new (P^N) AuCl complexes and their RedOx activity.

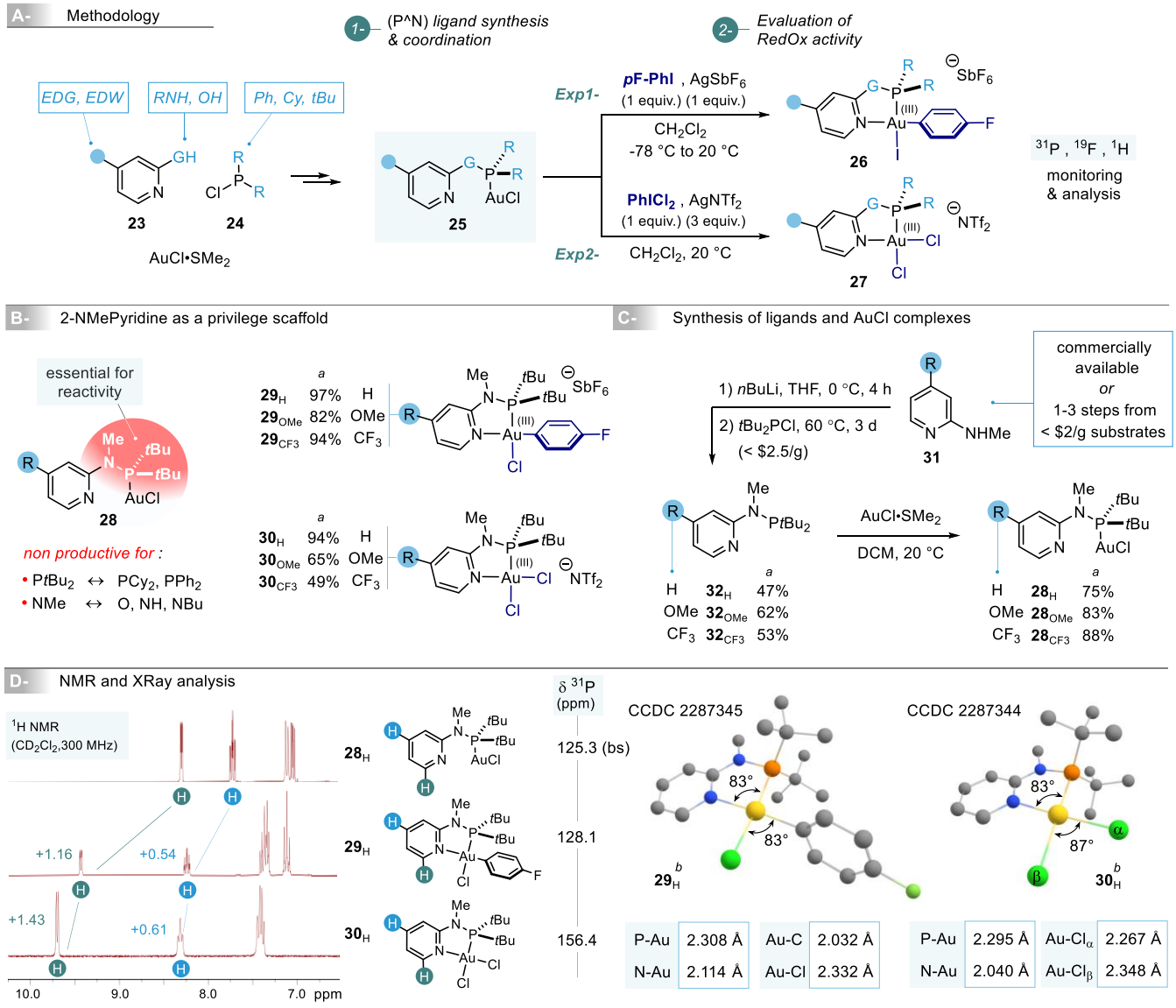

[a] Isolated yields. [b] H atoms and counteranion (SbF_6^- for $\mathbf{29}_H$ and Tf_2N^- for $\mathbf{30}_H$) omitted for clarity.

Interestingly, the P-Au bond is slightly longer (2.308 Å vs 2.270 Å) and the P-N bond shorter (2.114 Å vs 2.137 Å) for the pyridine-based complex $\mathbf{28}_H$, which also exhibits a smaller N-Au-P bite angle (83° vs 87°).The V_{Bur}%[24] of $\mathbf{28}_H$ was calculated[25] to be 45.8%, a value below that of MeDalPhos (49.6%) that may be the result of the planarity of the pyridine N donor and could potentially translate into a more favorable access to the Au(III) center during catalytic events.

Catalytic reactivity. The catalytic reactivity of the new pyridine-based (P^N) Au(I)Cl complexes **28** was then evaluated. To this purpose, the intramolecular alkoxy- and amidoarylation of alkenes, previously reported independently by the groups of Bourissou and Patil were chosen as model reactions (Figure 3-A).[9e,g] The reason for such a choice stands in the specificity of the transformation which capitalizes both on the RedOx properties of Au(I) complexes for the activation of Ar-I bonds and on the Lewis acid reactivity of Au(III) species for the nucleophilic functionalization of p systems. The mechanism proposed for this transformation is shown in Figure 3-B.[8,26] In addition, a large reaction scope has been reported with the (MeDalPhos)AuCl complex that would allow for an appropriate comparative evaluation of the catalytic potential of the new (P^N) AuCl complexes **28**.

Figure 3. Catalytic tests.

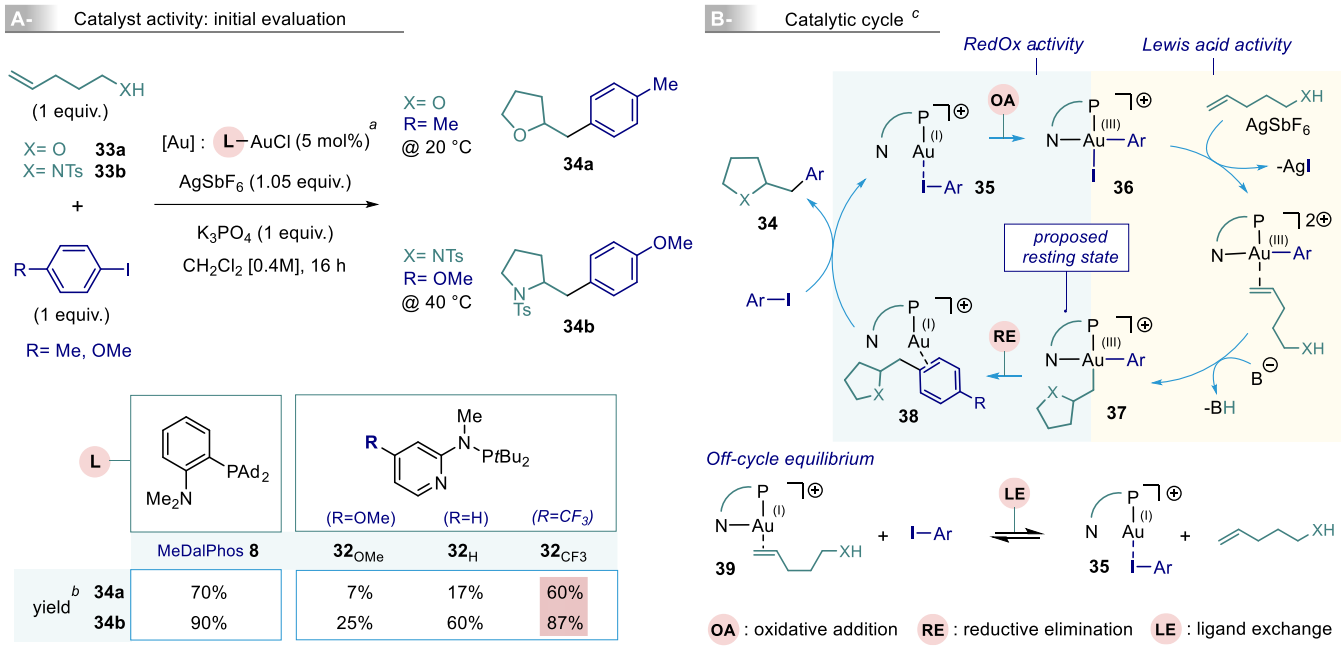

[a] Reactions performed at 0.05-0.1 mmol scale using screw-cap vials and an oil bath with temperature regulation. [b] Yield determined by ^{1}H NMR spectroscopy analysis of the crude reaction mixture using mesitylene as an internal standard. [c] see ref 26.

Experimental conditions from the literature[9e,g] were directly employed in an attempt to accessing furan derivative **34a** and pyrrolidine derivative **34b**. When MeDalPhos was used as the ligand, yields similar to those reported in the literature were obtained Figure 3-A.[9e,g] We were pleased to see that **34a** and **34b** could also be produced when ligands **32** were employed but the efficiency of the transformations was largely dependent on the nature of the substitution on the pyridine moiety. The use of ligands **32**$_H$ and **32**$_{OMe}$ with respectively no substitution or with a OMe group at position C(4) led to the inefficient formation of **34a** (7% and 17%, respectively). In contrast, ligand **32**$_{CF3}$ with a *p*-CF_3 substituent allowed for a largely improved reactivity (**34a**: 60% yield) that is comparable to that observed when MeDalPhos is employed (70%). The same trend was observed for the synthesis of pyrrolidine **34b**. In this case, very comparable yields were obtained when **32**$_{CF3}$ (87%) and MeDalPhos (90%) were used, while **32**$_H$ allowed for the production of **34b** with a more moderate efficiency (60%). These seminal results were found promising in light of the very limited number of ligands available for Gold(I/III) RedOx catalysis and the modulation of reactivity that could be easily achieved by simply modifying the substitution pattern of the pyridine moiety. An obvious trend came out from analyzing the results of these preliminary catalytic tests: the more electron poor the pyridine moiety, the better the yield in reaction products. The presence of substituents on the pyridine would affect its Lewis basicity and therefore the way it would interact with the gold center, what would ultimately impact the stability of the catalytic species along the reaction pathway. According to DFT calculations performed by Miqueu and Bourissou using MeDalPhos as the ligand, **33a** and PhI as substrates,[26] the portion of the transformation relying on the Lewis acid reactivity of the catalyst (**36**→**37**) (see Figure 3-B) is highly exergonic and exhibits a low activation energy demand ($\Delta G^{\neq}$ cyclization < 3 kcal.mol^{-1}). The oxidative addition (OA) was also calculated to be largely accessible ($\Delta G^{\neq}_{\mathbf{35}\rightarrow\mathbf{36}}$= 11.2 kcal.mol^{-1}), while the reductive elimination step (RE) was proposed to be rate determining ($\Delta G^{\neq}_{\mathbf{37}\rightarrow\mathbf{38}}$= 17.9 kcal.mol^{-1}). These computational and analytical data are in line with the substitution effect observed when the catalytic activity of complexes **28**$_{H,OMe,CF3}$ were assessed. Provided that it does not severely impact the other steps of the reaction, the use of a more electron poor ligand (like **28**$_{CF3}$) would be beneficial as it would allow lowering the energy barrier of the RE step.

Computational study and ligand optimization. To get more insight into how the substitution of the pyridine moiety in ligand **32** can affect the reaction, and with the goal of developing more efficient catalytic systems, a computational study was performed (Figure 4-A). The reaction between pentenol **33a** and PhI was examined and, to have a broader view on the ligand substitution effect, three steps were considered: the reductive elimination (RE, see **37**→**38**, Figure 3-B), the oxidative addition (OA, see **35**→**36**, Figure 3-B), and

the pentenol to PhI ligand exchange at the Au(I) center (LE, see **35**→**39**, Figure 3-B). This exchange, which is an off-cycle equilibrium, was considered to possibly affect the reaction depending on the experimental conditions employed.[27,10b,10c] calculations were conducted with ORCA 5.0.2[28] at the PWPB95-D4/def2-TZVPP + SMD(CH_2Cl_2) // R^2SCAN-3c level of theory,[20] which, following recent papers on the subject,[29] was considered to be a good compromise between computational effort and accuracy. Dispersion (D4) and solvent effects (CH_2Cl_2) were taken into account. The same series of calculations ($\Delta G^{\neq}$ and ΔG for RE and OA, ΔG for LE) were performed using either MeDalPhos, **32**$_{OMe}$, **32**$_{H}$ or **32**$_{CF3}$ as the ligand and the data were compared (Figure 4-A, Tab1). With MeDalPhos, energy values in adequation with those previously reported were obtained, thus validating the method employed. For instance, the ($\Delta G^{\neq}$, ΔG) set of energies for the RE step was calculated to be (17.4, -25.4 kcal.mol^{-1}), in good agreement with the data reported by Miqueu and Bourissou (17.9, -24.7 kcal.mol^{-1}).[26] As expected, the RE activation barrier gradually decreases (while the exergonicity increased) when the pyridine moiety becomes more electron poor (Figure 4-A, Tab1). A $\Delta\Delta G^{\neq}$= 2.4 kcal/mol^{-1} was found when comparing the data for the extremal **32**$_{OMe}$ and **32**$_{CF3}$ ligands. This value may account for the difference of reactivity observed during the catalytic tests (Figure 3-A).

Figure 4. DFT-guided ligand optimization and catalytic evaluation.

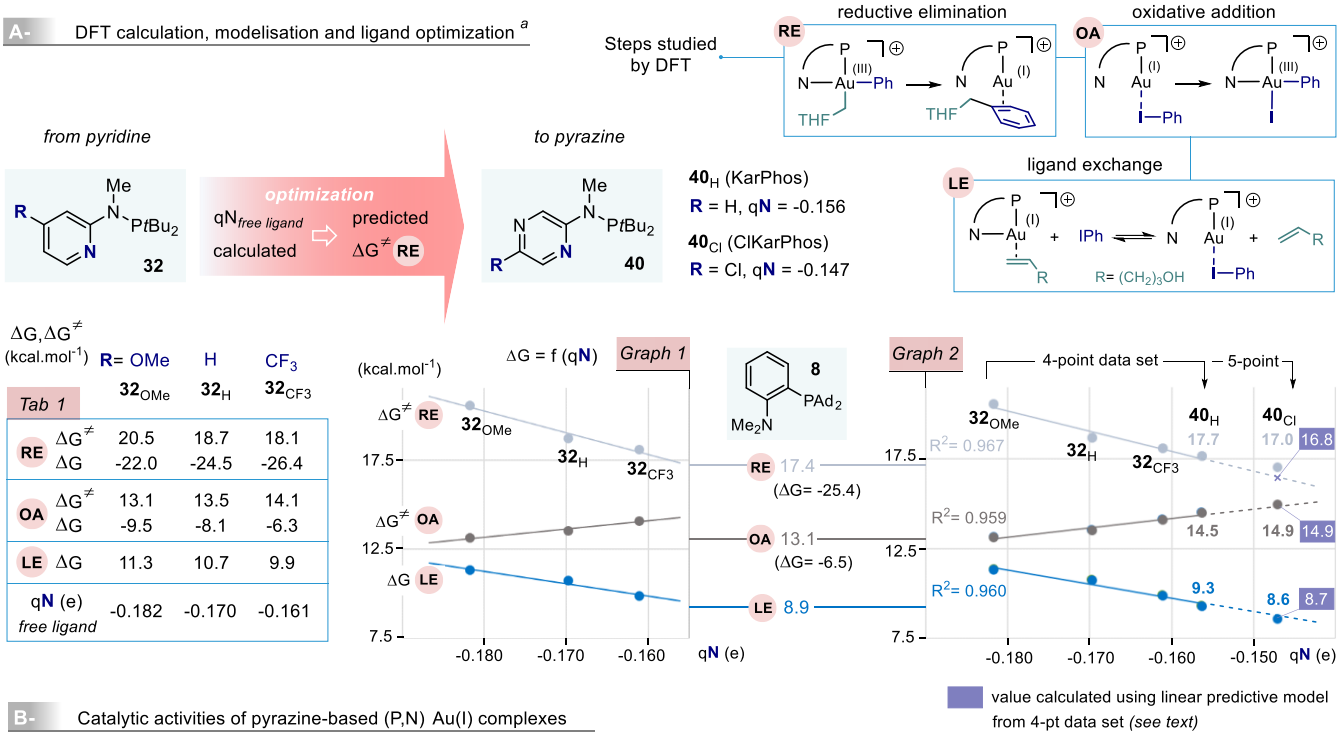

[a] DFT calculations performed at the PWPB95-D4/def2-TZVPP + SMD(CH_2Cl_2)//R^2SCAN-3c level of theory, see Supporting Information for more detail. [b] Reactions performed at 0.05-0.1 mmol scale using screw-cap vials and an oil bath with temperature regulation. [c] Yield determined by ^{1}H NMR spectroscopy analysis of the crude reaction mixture using mesitylene as an internal standard. [d] AgOTf was employed.

Logically, the opposite effect was observed for the OA step, that was calculated to be both more accessible and more exergonic when making the pyridine core more electron rich. Notably, the electronic effect induced by the substitution appeared to be less pronounced for the OA than for the RE ($\Delta\Delta G^{\neq}$= 1.0 kcal.mol^{-1}, $\Delta G^{\neq}$(**32**$_{OMe}$) versus $\Delta G^{\neq}$(**32**$_{CF3}$)). As for the LE step, the stability of the Au(I)-pentenol complex **39** decreases with ligands possessing a more electron poor pyridine moiety.[10c] This evolution reflects the involvement of the pyridine N atom in the stabilization of the π-complex **39** by coordination,[27] an effect not in play for complex **35**. While **32**$_{CF3}$ led to a promising result during the catalytic tests (Figure 3-A), these DFT calculations also demonstrate that, when compared to the series of ligands **32**, the use of MeDalPhos allows for the lower RE and OA energy barriers, and the most favorable LE equilibrium.

In an effort to correlate the calculated variation in energy ($\Delta G^{\neq}$, ΔG for RE, OA and LE) with the nature of the substituents on the pyridine moiety, we looked for a parameter that could reflect the change in the pyridine electronics and its resulting modified interaction with the gold center. Since the pyridine moiety coordinates to Au *via* the N atom, we hypothesized that the charge on this atom (qN) could be a suitable descriptor of the substituent effect and ideally an appropriate predictor of the reaction barrier heights and energies. To this end, the structures of the free ligands **32**$_{OMe}$, **32**$_{H}$ or **32**$_{CF3}$ were optimized and the Hirshfeld charge at the N$_{pyr}$ atom (qN) calculated for each of them.[20] These data are compiled in Tab1 of Figure 4-A. Interestingly, when plotting the $\Delta G^{\neq}$ of the OA and RE steps, and the ΔG of the LE step as a function of qN, some linear correlations seem to shape (Figure 4-A, Graph1). Similar correlations (not shown in Graph1) were obtained for the ΔG of the OA and RE steps.[20] Given the minimal set of data, and with the idea to design new and more efficient catalysts, we decide to confront this emerging model with additional data calculated for a new ligand. The unreported pyrazine-based (P^N) ligand **40**$_{H}$ (KarPhos) was considered an appropriate candidate. The pyrazine moiety was expected to possess a reduced coordination ability as compared to the 4-CF$_3$-pyridine[30] what should translate in a lower $\Delta G^{\neq}$ for the RE step. The structure of KarPhos (**40**$_{H}$) was optimized in silico and the Hirshfeld charge at the N atom calculated, providing indeed a lower value than for **32**$_{CF3}$ (Figure 4-A). Then, the barrier heights and energies for the RE, OA and LE steps were calculated, and the values plotted along with those previously obtained for the pyridine-based (P^N) ligands **32**. Gratifyingly, we found the new set of data to reinforce the suspected correlation and therefore the possibility to use the qN Hirshfeld charge as an efficient predictor (Figure 4-A, Graph2). The model build with the 4-point data set was tested with an additional ligand, ClKarPhos (**40**$_{Cl}$) considering that the electron withdrawing chlorine atom introduced on the pyrazine moiety at C(5) would make the RE even more favorable.[31] A similar in silico process was employed to determine after structural optimization that the qN value was the lowest calculated so far (qN= -0.147 e, Figure 4-A). This value was employed to predict the barrier heights and energy of the reaction using the linear model derived from the 4-point data set (Figure 4-A, Graph2). Remarkably, these predicted values were found to deviate by less than 2% from the values calculated by DFT calculation, a process that was obviously far more demanding in time and resources. From a reactivity point of view, the DFT-guided designed ligands KarPhos (**40**$_{H}$) and ClKarphos (**40**$_{Cl}$) should, according to the calculations, be at least competitive to MeDalPhos for the model reactions studied. ClKarPhos even provided the lowest $\Delta G^{\neq}$ for the key RE step (17.0 kcal.mol^{-1} vs 17.4 kcal.mol^{-1} for MedalPhos). The minimization of this barrier height could be made in exchange to a more energy demanding OA, which remains comparatively easier (14.9 kcal.mol^{-1}). To validate our optimization approach and the data produced in silico, ligands **40**$_{H}$ and **40**$_{Cl}$ were synthesized following a route analogous to that previously employed for the pyridine-based ligands **32** (Figure 2-C). The process was efficient and amenable to multigram scale synthesis starting from readily available pyrazine building blocks (Figure 5). The corresponding AuCl complexes were produced in very good yield from **40**$_{H}$ and **40**$_{Cl}$.

Figure 5. Synthesis of (P^N) ligands KArPhos (**40**$_{H}$) and ClKarPhos (**40**$_{Cl}$) and the corresponding AuCl complexes

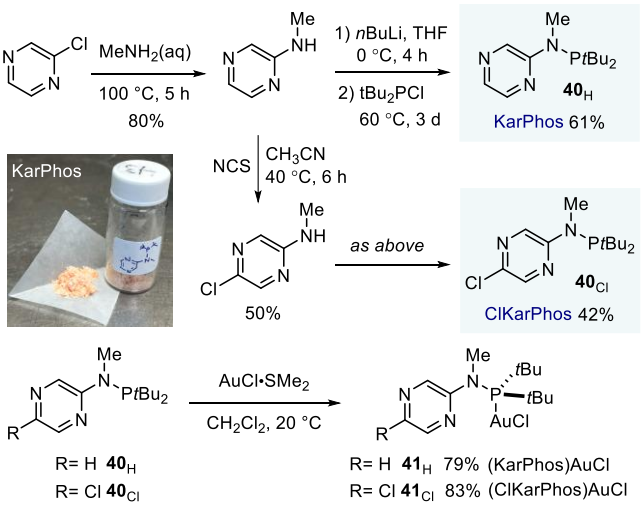

The catalytic activity of complexes **40**$_{H}$ and **40**$_{Cl}$ was first assessed in the model reactions leading to **34a** and **34b**. The results of these experiments are provided in Figure 4-B. Not only these DFT-guided designed complexes were shown to be more efficient precatalysts than those based on the use of pyridine-based ligands, but they also equaled or outperformed (MeDalPhos)AuCl. Furan **34a**, whose formation served as a model for the ligand optimization, was produced

in an improved 84% yield in the presence of (ClKarPhos)AuCl (**40**$_{Cl}$), (+14%) while the formation of pyrrolidine **34b** was almost quantitative (98%). The same trend was observed over three additional examples of alkoxy or amidoarylation of alkenes (**34c-e**) thus demonstrating the catalytic potential of **40**$_{H}$ and **40**$_{Cl}$ for such type of reactions. It is interesting to note that, according to the predictive model (Figure 4-A, Graph2), the $\Delta G^{\neq}$ of the RE step could still be reduced provided that an appropriate heteroaromatic motif allowing a lower qN of the ligand could be found. However, this optimization has some limit which should be reached when the $\Delta G^{\neq}$ of the OA step would equal that of the RE step. An optimum value of $\Delta G^{\neq}$= 15.6 kcal.mol^{-1} for qN= -0.135 e is proposed by the model.

Exploring the catalytic potential of new (P^N) Au(I) complexes in C-S bond formation processes. Given the remarkable efficiency demonstrated by complexes **40**$_{H}$ and **40**$_{Cl}$ in the alkoxy- and amidoarylation of alkenes, it was decided to further explore their potential as catalysts to achieve more challenging transformations.

Figure 6. Thiosulfonylation of aryl iodides: from concept to feasibility.

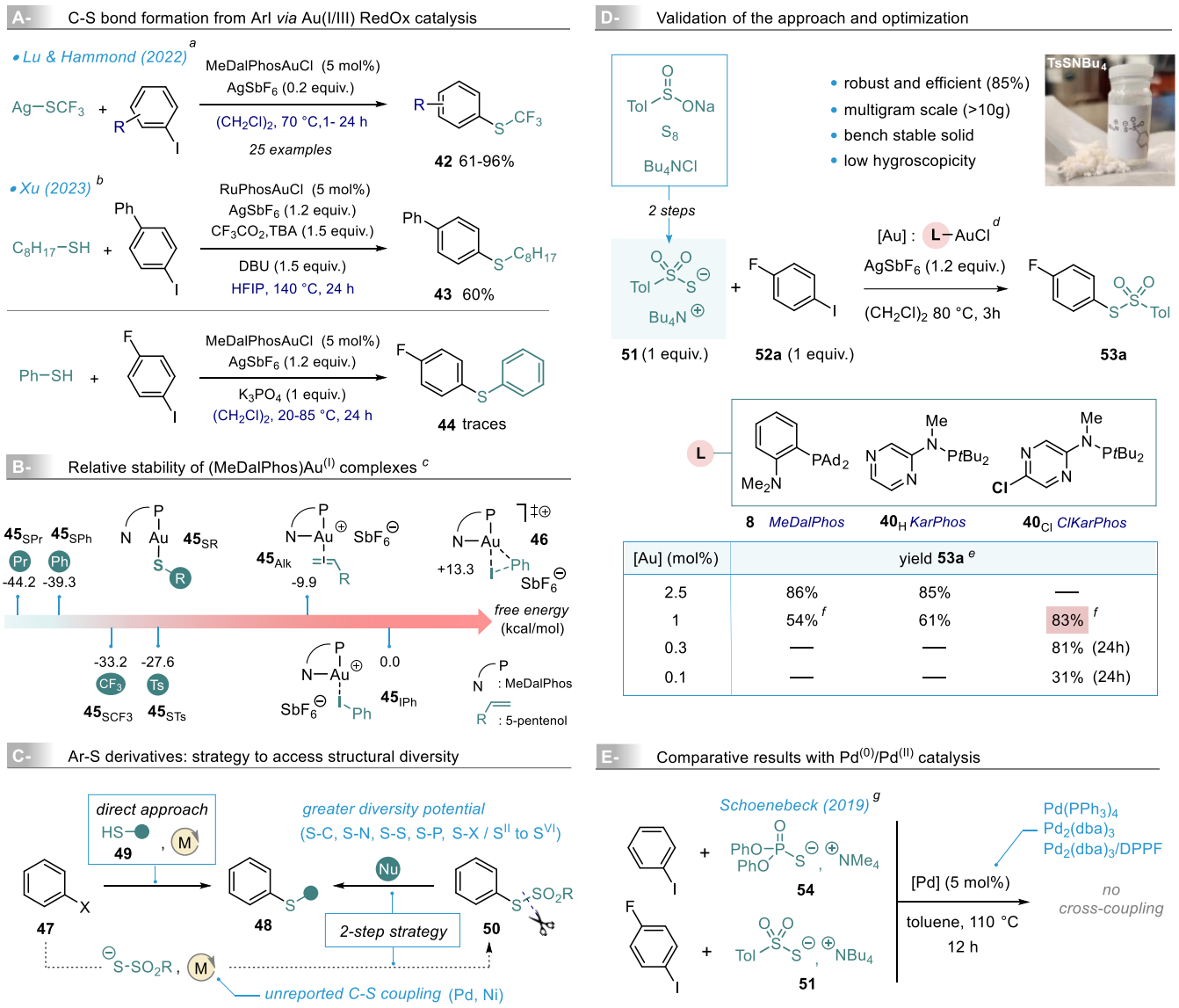

[a] see ref 9n. [b] see ref 6b. [c] DFT calculations performed at the PWPB95-D4/def2-TZVPP + SMD(CH_2Cl_2)//R^{2}SCAN-3c level of theory, see Supporting Information for more detail. [d] Reactions performed with screw-cap vials using an oil bath with temperature regulation and >700rpm stirring. [e] Yield determined by ^{1}H NMR spectroscopy analysis of the crude reaction mixture using mesitylene as an internal standard. [f] average yield for a triplicate experiment. [g] see ref 42.

We turned out our attention on the catalytic formation of C-S bonds by cross-coupling of aryl iodides with sulfur derivatives. The stoichiometric reaction between cyclometalated Au(III) complexes and thiols was initially described by Leung and Wong in the context of cysteine residues bioconjugation.[32] The concept was further developed and exploited by Spokoyny and collaborators for the chemoselective structural modification of proteins and sugars with aryl gold(III) complexes bearing bidentate (P^N) ligands.[33] The group of Bochmann also reported the stoichiometric reaction of (C^N^C)Au(III) pincer complexes with adamantly thiol, showing the capacity of the resulting Au(III) thiolates to generate C-S bonds by reductive elimination.[34] The first instance of C-S bond formation under catalytic conditions was reported by Shi and coworkers using aryldiazonium salts and a cysteine derivative in the presence of Ph_3PAuCl.[35] Lu and Hammond recently described that less hazardous and structurally more varied aryl iodides could be employed as substrates in the catalytic formation of aryl trifluoromethylthioethers **42** (Figure 6-A).[9n] The comparatively more energy demanding C-I bond oxidative addition step could be achieved using MeDalPhos as the ligand. However, the rather mild experimental conditions employed in this transformation appear to be specific to the formation of C-SCF_3 bonds. The cross-coupling with a simple alkyl thiol was attempted by Xu and coworkers and was shown to require more forcing conditions (additives, 140 °C, 24 h, see Figure 6-A).[6b] Despite its moderate efficiency (60%), the formation of **43** remains to date, the only example of a gold-catalyzed cross-coupling of an aryl halide with an alkylthiol. Our attempts to produce **44** by reaction between thiophenol and 4-fluoroiodobenzene using experimental conditions commonly employed in Au(I/III) redox catalysis failed (Figure 6-A).[9c] The difficulty to form C-S bonds under Au(I/III) redox catalysis using thiols as reaction partners could be associated with the high thiophilicity of gold species and the resulting stability of thiolate-Au(I) complexes.[36] During a catalytic process, the formation of such complexes would compete with the coordination of the Au(I) catalyst to the aryliodide, a requisite event prior to the oxidative addition step.

To evaluate such a possibility, the free energies of a series of MeDalPhos-gold(I) complexes **45** bearing various ligands were computed (Figure 6-B).[20] The PhI-coordinated Au(I) complex $\mathbf{45}_{PhI}$ was chosen as the reference and the relative stabilities of the other complexes **45** were assessed by calculating the ΔG of the corresponding ligand exchange reactions.[20] Notably, thiolate complexes $\mathbf{45}_{SPh}$ and $\mathbf{45}_{SPr}$ were found to be more stable than $\mathbf{45}_{PhI}$ by ≈40 kcal.mol^{-1}, thus rendering the direct ligand exchange between thiolates and phenyl iodide inaccessible. Comparatively, the Au(I)-pentenol π-complex $\mathbf{45}_{Alk}$ was calculated to be only 9.9 kcal.mol^{-1} lower in energy than $\mathbf{45}_{PhI}$, thus allowing the ligand exchange and subsequent oxidative addition step to take place at room temperature (overall Ea= 23.1 kcal.mol^{-1}). This value agrees with the experimental evidence reported by Bourissou and coworkers that oxidative addition slowly proceeded when (MeDalPhos)Au(I)-octene complex was reacted at 20 °C with a stoechiometric amount of PhI.[9e] We found that this reaction could be largely accelerated (> 90% conversion after 0.5 h) when 1 equiv. of $AgSbF_6$ was added to the mixture.[20] This silver effect, which can be attributed to the competitive coordination of Ag+ to the alkene, should also be in play in the trifluoromethylthiolation of aryl iodides (Figure 6-A), as suggested by Lu and Hammond.[9n] Despite the significant difference in thermodynamic stability between Au(I)-SCF_3 complex $\mathbf{45}_{SCF3}$ and $\mathbf{45}_{PhI}$ (≈33 kcal.mol^{-1}, see Figure 6-B), the oxidative addition step could remain accessible in the presence of excess Ag+ salts since these ones could compete with the gold(I) complex for coordination to the SCF_3 moiety. DFT calculations support this hypothesis (equation 1): in the presence of $AgSbF_6$, the thiolate/PhI exchange was found to be thermodynamically less unfavorable (≈11.7 kcal.mol^{-1}) (see section on mechanistic investigations for additional information).

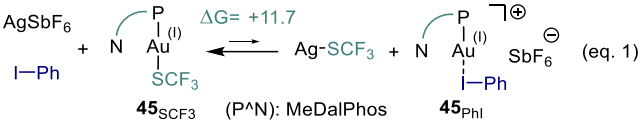

In this context and following the above considerations, we design a new approach to the synthesis of aryl sulfur derivatives **48** (Figure 6-C). These important structural motifs are commonly produced by C-S bond forming process *via* a direct metal-catalyzed cross-coupling between an activated aryl derivative **47** and the corresponding sulfide **49**.[37] Such an approach has several significant limitations mostly associated with the use of **49**. First, the number of commercially available R-SH building blocks is limited, which may require their synthesis prior to the coupling and second, they are notoriously malodorous in their great majority thus making their use on large scale unpractical. In addition, thiols can be readily oxidized into disulfides and are therefore air-sensitive compounds. Finally, the method is generally restricted to the use of RSH coupling partner where R is a carbon-based substituent, which limits the structural motifs that can be produced. Our strategy to access aryl sulfur derivatives **48** (Figure 6-C) is based on a two-step sequence that involves 1- an initial cross-coupling of an Ar-I with an amphiphilic thiosulfonate derivative RSO_2S^-, followed by 2- a functionalization of the resulting arylthiosulfonate intermediate **50** by umpolung at the S center. While having an additional step, this approach could allow for a greater structural diversity with the possibility to employ a variety of nucleophilic partners during the functionalization step. The formation of *S*-arylthiosulfonate of type **50** by C-S bond formation is an

unclassical approach[38] and very limited work has been made in this area.[39] Very surprisingly, and to the best of our knowledge, the coupling of an aryl halide with a thiosulfonate has never been explored. Boehringer Ingelheim Pharmaceuticals researchers reported in 2014 a Cu(I)-catalyzed cross-coupling of aryl iodides with sodium thiosulfate to produce $ArSSO_3Na$ Bunte salts, which represents to date the only example of metal-mediated coupling with a thiosulfonyl moiety (equation 2).[40] While efficient, the method requires high loading of catalyst (10 mol%), had limited exemplification and the $ArSSO_3Na$ Bunte salts could only be obtained in 50-70 wt.% purity as the result of the isolation protocol.

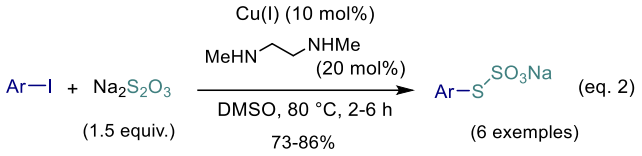

Figure 7. Scope of the Au-catalyzed cross-coupling reaction of aryl iodides with ammonium thiotosylate.

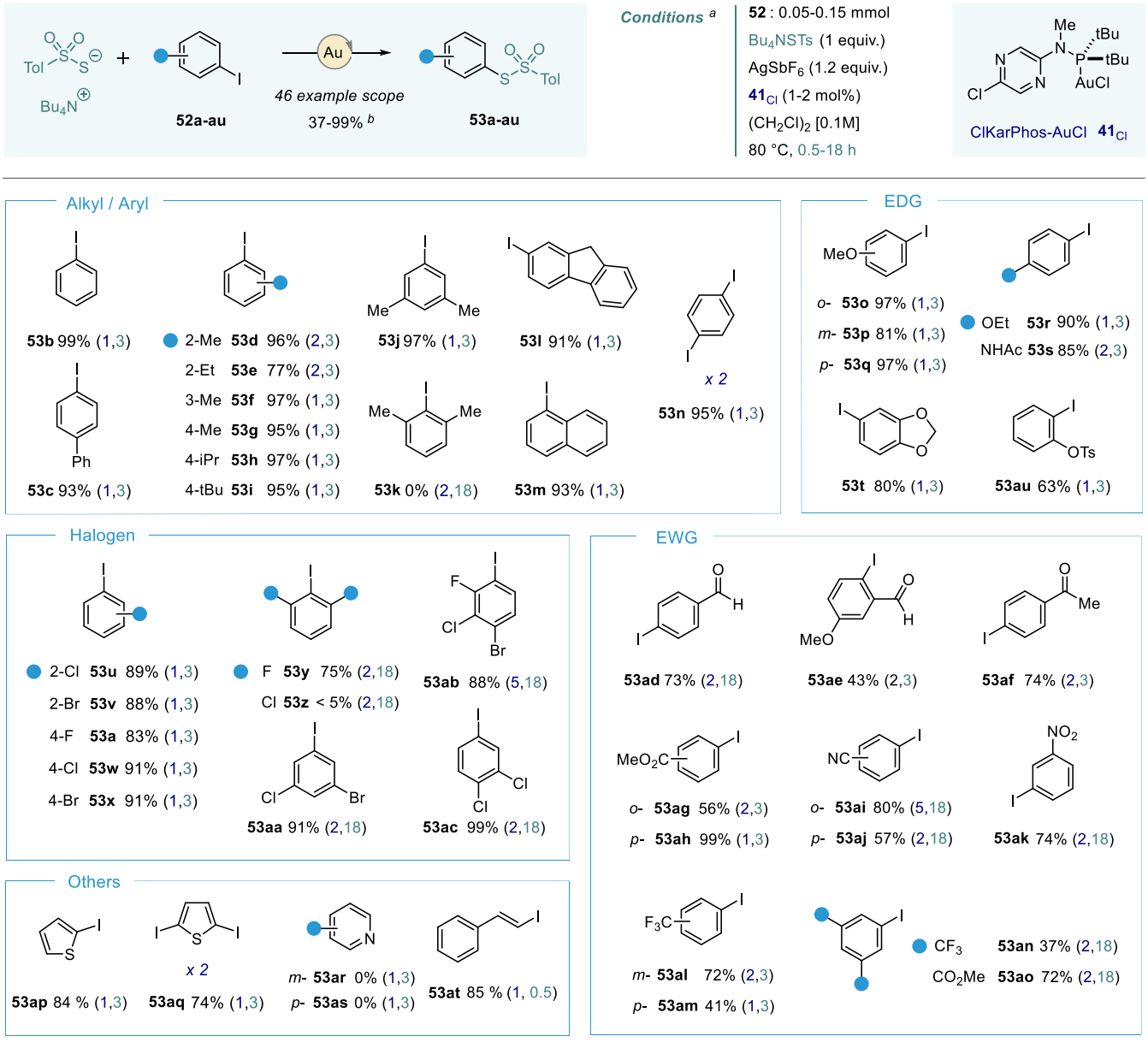

[a] Reactions were performed with screw-cap vials using an oil bath with temperature regulation and >700rpm stirring, see Supporting Information for details. For each substrate the catalyst loading (mol%), and the reaction time (h) are sequentially provided between brackets. [b] Yields were determined by ^1H NMR spectroscopy analysis of the crude reaction mixture using mesitylene as an internal standard.

We considered that a thiotosylate anion could be an appropriate coupling partner for our approach. This choice was motivated by the ease of access to such species and the calculated greater lability of the TsS moiety in the corresponding MeDalPhosAu(I)STs complex **45**$_{STs}$ as compared to other thiolate Au-(I) complexes **45**$_{SR}$ (Figure 6-B). More specifically, the STs complex **45**$_{STs}$ was found 5.6 kcal.mol^{-1} less stable than the SCF_3 one (**45**$_{SCF3}$) what was considered as a favorable factor for the targeted cross-coupling reaction. The tetrabutylammonium thiotosylate salt **51** (Bu_4NSTs) could be easily produced in a 2-step sequence using inexpensive starting material ($TolSO_2Na$, S_8 and TBAC) (Figure 6-C). The sequence was efficient (85% overall yield), could be performed on a multigram scale and **51** appeared to be a bench stable solid with low hygroscopicity. The cross-coupling was attempted using stoichiometric amounts of **51** and 4-F-iodobenzene **52a**, 1.2 equiv. of $AgSbF_6$ as halide scavenger[41] and ligand exchange facilitator, in DCE at 80 °C. When 2.5 mol% of (MeDalPhos)AuCl complex was employed as pre-catalyst, we were pleased to observe that the desired aryl thiotosylate **53a** was produced in 86% yield after 3 h of reaction (Figure 6-C). Gratifyingly, the use of the Karphos ligand (**40**$_H$) led to a similar outcome (**53a**: 85%). When the catalyst loading was reduced to 1 mol%, a slightly better result was obtained with **40**$_H$ (61% versus 54%). However, ClKarPhos (**40**$_{Cl}$) was found to be an optimum ligand for this transformation, allowing the formation of **53a** in a largely improved 83% yield. This remarkable result, which was confirmed by triplicate experiments, attests of the potential of the newly designed (P^N)-Au(I) complexes for RedOx catalysis. The success encountered with the use of the ClKarPhos allowed for a reduction of the catalyst loading down to 0.3 mol% without noticeable loss of efficiency (81% yield, 24 h). At 0.1 mol%, a 310 TON could be obtained, what, to the best of our knowledge, represent the highest TON value for a such a type of Au-mediated RedOx process. For comparison, at lower loading than 5 mol% of (MeDalPhos)AuCl, the trifluoromethylthiolation reported by Hammond and Lu (Figure 6-A) was found far less efficient (32%, 2 mol%).[9n]

Finally, we rapidly evaluate the possibility to perform the reaction using Pd-catalysis. Similarly, to what was previously reported by Schoenebeck and coworkers for the cross-coupling of aryl iodides with Phosphorothiolate **54** (Figure 6-E),[42] the reaction could not be performed under Pd(0)/Pd(II) catalysis using classical experimental conditions. This result highlights the singular catalytic potential of Au(I) complexes in such a type of transformations.

Reaction scope and applications. The scope of the transformation was then evaluated (Figure 7). A variety of aryl iodides (46 representative examples) were treated under the optimized conditions using generally 1-2 mol% of complex **41**$_{Cl}$. Alkyl, halogen, EDG and EWG substituents were well tolerated. Yields were found to be largely independent of the nature of the substituent (81% average yield). Multiple substitution was tolerated at any position of the aromatic (ortho, meta, para) but a limit in reactivity was reached for di-*ortho*-substituted aryl iodide bearing sterically demanding group/atoms. (see for instance **53k** and **53z** versus **53y**).

Figure 8. Structural diversification *via* post-transformations on arylthiotosylate **53a**.

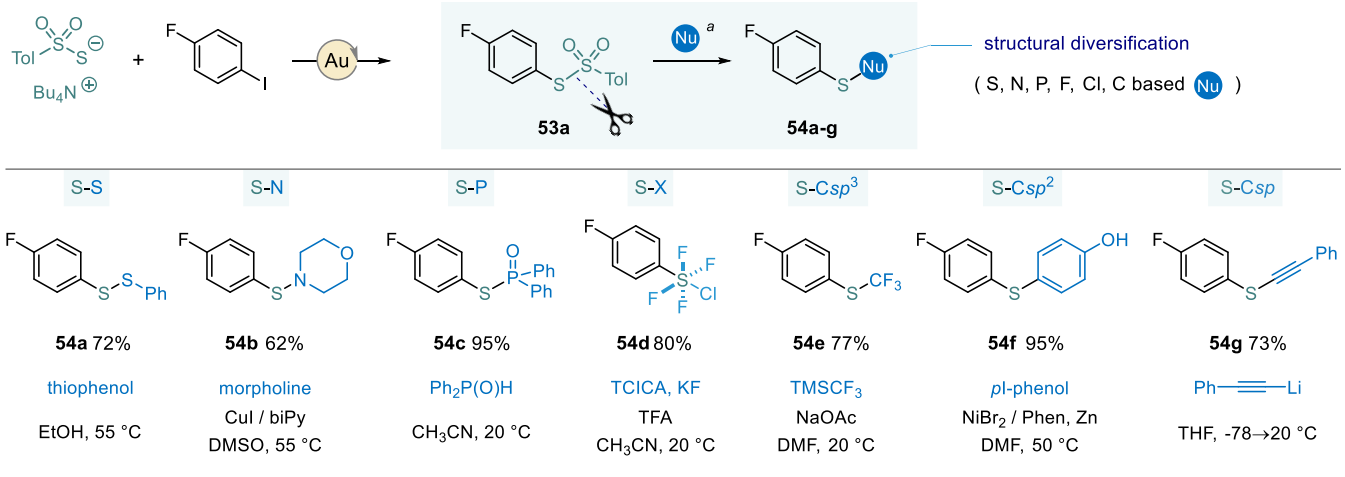

[a] See Supporting Information for details on the experimental procedures.

A remarkable chemoselectivity was observed for aryl iodides possessing different halogen atoms (F, Cl, Br). The examples of aryl iodides **52aa** and **52ab**, which possess 3 and 4 different halogens respectively, are particularly representative. Thiotosylates **53aa** and **53ab** resulting from an exclusive cross-coupling at the C-I position were formed in excellent yield (91% and 88%, respectively). As for EWGs, ester, aldehyde, ketone, cyano, nitro and trifluoromethyl substituents were all tolerated. A 2 mol% catalyst loading was generally required to achieve high conversion of the substrates. The reaction was found easier to perform in the case of aryl iodide possessing EDGs: 1 mol% of **41**$_H$ and 3 h of reaction allowed for yields in cross-coupling products higher than 80%. While the reaction could not be performed onto pyridines (see **53ar** and **53as**), it was efficient with thiophenes (see **53ap** and **53aq**). Multiple cross-couplings could be realized on poly-iodo derivatives as attested by the formation of compounds **53n** and **53aq**. Finally, the reaction of b-iodostyrene **52at**, which delivered compound **53at** in a rapid, efficient, and stereospecific manner (85%, *E* isomer, 0.5 h), attests that the cross-coupling has the potential for the functionalization of other Csp^2-I bonds.

To conclude with our 2-step strategy, thiotosylate **53a** was reacted under a variety of conditions allowing the cleavage of the S-Ts bond with concomitant functionalization at the S center (Figure 8). A small library of products could be generated by directly using procedures from the literature or by adapting reported protocols.[20] New S-Csp^3, -Csp^2 and -Csp bonds could be formed by addition of organometallics, Ni-catalyzed cross-coupling or by simple nucleophilic substitution (see **54e-g**). S-Heteroatom bond formation was also amenable as attested by the production of disulfide **54a** (72%), sulfenylamine **54b** (62%) and thiophosphinate **54c** (95%). Finally, the valuable SF_4Cl derivatives **54d** was produced in 80% by adapting a procedure reported by the Cornella group for the conversion of somewhat related aryl phosphorothiolate substrates.[20] Notably, among the derivatization products obtained, a large number could not be directly produced by metal-catalyzed cross coupling reaction of an aryl halide with the corresponding R-SH derivative.

Mechanistic investigations. To get more insight into the mechanism of the reaction, a series of computational and experimental studies were conducted. The results of these investigations are summarized in Figure 9. DFT calculations were performed with ORCA 5.0.2 at the PWPB95-D4/def2-TZVPP + SMD(1,2-dichloroethane) // R^{2}SCAN-3c level of theory, using ClKarPhos (**40**$_{Cl}$) as the ligand and Et_4N^+ as a model for Bu_4N^+.[28,29] The oxidative addition step (**55**→**56**) was found to have a moderate energy of activation ($\Delta G^{\neq}$= +14.9 kcal.mol^{-1}) and to be slightly exergonic (ΔG= -4.1 kcal.mol^{-1}) (Figure 9-A). The subsequent I to STs ligand exchange by reaction of **56** with AgSTs was calculated to be slightly favorable by 1.6 kcal.mol^{-1}. It was considered that the thiophilic $AgSbF_6$ species would easily react with Et_4NSTs, to produce AgSTs and Et_4NSbF_6, an assumption that is supported by calculation (ΔG= -25.7 kcal.mol^{-1}). The reductive elimination step (**57**→**58**) was found more energy demanding ($\Delta G^{\neq}$= +19.8 kcal.mol^{-1}) than the oxidation step and more exergonic (ΔG= -11.5 kcal.mol^{-1}). The catalytic cycle could be closed by TsS-Ph to PhI ligand exchange at the Au(I) center (**58**→**55**), a step that was found to be uphill (ΔG= +4.8 kcal.mol^{-1}).[43] Alternatively, Au(I) species **58** most likely reacts with AgSTs to produce the Au(I)-thiotosylate complex **60**.[44] Intermediate **60** appears to be a thermodynamic sink (26.2 kcal.mol^{-1} more stable than **55**, a value comparable to that calculated for the (MeDalPhos)Au(I) complex, see Figure 6-B) and was detected by ESI-HRMS analysis of a running reaction as the catalyst resting state. The Ag+ mediated off-cycle equilibrium between **60** and **55** appears to be primordial to the success of the cross-coupling reaction.

Figure 9. Mechanistic studies and proposed catalytic cycle for the Au$^{(I)}$/Au$^{(III)}$-mediated thiosulfonylation of aryl iodides.

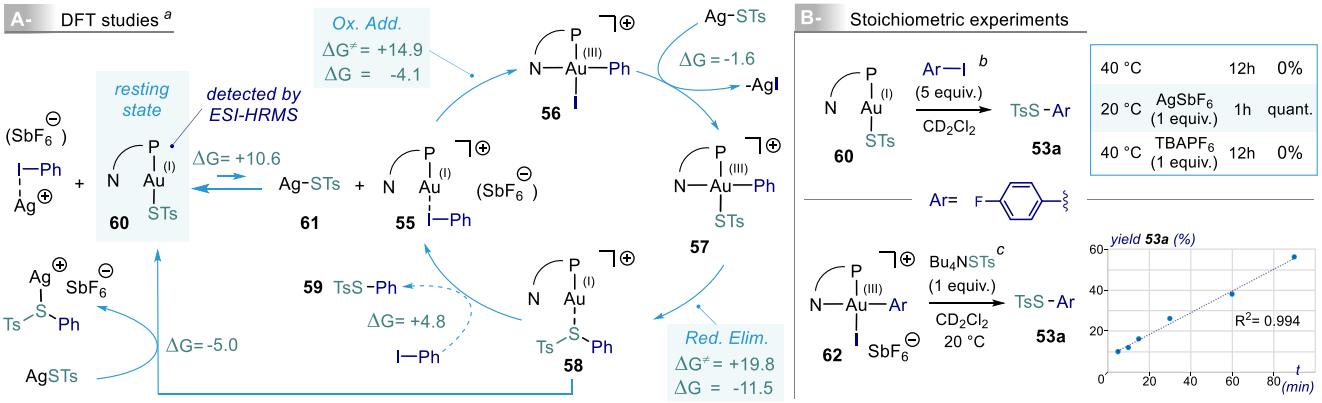

a DFT calculations performed at the PWPB95-D4/def2-TZVPP + SMD(1,2-dichloroethane)//R^{2}SCAN-3c level of theory, see Supporting Information for more detail. (P^N)= ClKarPhos. b Reaction monitored by ^{1}H, ^{31}P and ^{19}F NMR analysis; (P^N)= ClKarPhos. c Reaction monitored by ^{31}P and ^{19}F NMR analysis; (P^N)= MeDalPhos.

$AgSbF_6$ has a dual role in the transformation: not only it acts as an iodide scavenger, but it also allows for the reduction of the energy required to access **55**.As a consequence, $AgSbF_6$ has to be used in slight excess (1.2 equiv.) to ensure that it is not initially fully converted into AgSTs since "free"[45] Ag+ is required for the TsS to PhI exchange at the Au(I) center (**60**→**55**). The role of the silver salt was confirmed by a stoichiometric reaction in which Au(I)-STs complex **60** was reacted with an excess of 4-fluoro iodobenzene (Figure 9-B). In the absence of $AgSbF_6$, the catalytic cycle could not be initiated, whatever the temperature and the reaction time, as the result of the difficulty to perform the required STs to PhI exchange. The same reaction performed with 1 equiv. of $AgSbF_6$ led to the quantitative formation of the Ar-STs cross-coupling product **53a** after only 1 h of reaction at 20 °C. A control experiment showed that the Ag+ salt was key to achieve such a reactivity: the use of the tetrabutylammonium salt $TBAPF_6$ could not trigger the RedOx process. It was also demonstrated that the role played by $AgSbF_6$ in the off-cycle equilibrium was more important than its activity as iodide scavenger. In the absence of $AgSbF_6$, the Au(III) complex **62** could still react with Bu_4NSTs to ultimately produce the Ar-STs cross-coupling product **53a** (Figure 9-B).[46] The reaction was found to follow zero-order kinetics, the rate determining step being the reductive elimination (see **57**→**58** with 4-FPh instead of Ph). The ^{31}P NMR monitoring of the reaction showed that a fast equilibrium took place between **62** and the corresponding Au(III)STs substitution complex, as attested by the broadening of the P ligand signal and its slight shifting over the course of the reaction.[47] In summary, the kinetics and the overall efficiency of the transformation seem to be dictated by the off-cycle equilibrium between complexes **60** and **55**. Superstoichiometric amounts of the silver salt and aryl iodide would be beneficial, while excess of the thiotosylate coupling partner would be detrimental. The observed higher catalyst loadings and longer reaction times required to convert aryl iodides possessing EWGs (see Figure 7) could be linked to the lower stability of the corresponding κ-IAr-Au(I) complex[48] as compared to **55**, and the consequent greater ΔG for the off-cycle equilibrium.[49] The conclusions of this study with regard to the dual role of the silver salt and the parameters affecting the kinetics and efficiency of the reaction, are important points to be considered in the design of gold-catalyzed RedOx transformations, more especially when one or several of the reactants can strongly bind to the cationic LAu(I) complex.

CONCLUSION During our investigations, a new family of hemilabile bidendate (P^N) ligands possessing a distinct structure than MeDalPhos were discovered to enable the oxidative addition of Csp^2-I to Au(I) centers. The initial design which consisted of replacing the Me_2NPh fragment of MeDalPhos by a 2-NMe-pyridine motif to increase ligand hemilability, structural and electronic modulation capacity was found successful. The first set of ligands, which exhibited promising RedOx activity in the model alkoxy- and amidoarylation of alkenes, were refined and optimized using DFT computational studies. The Hirshfeld charge at the coordinating N_{pyr} atom, calculated on the free ligand, was shown to be an appropriate predictor of the $\Delta G^{\neq}$ of the rate determining reductive elimination step. Two pyrazine-based ligands, KarPhos and ClKarPhos, suggested by the *in silico* study to possess an improved reactivity, were indeed shown to equal or outperform MeDalPhos in the model reactions and a series of related alkene arylations. Notably, these ligands can be obtained at the gram scale in a straightforward manner and from relatively unexpensive building blocks. The synthetic potential and comparatively higher reactivity of these new ligands was further highlighted in the thiotosylation of aryl iodides, a challenging unreported metal-catalyzed C-S cross-coupling reaction. Remarkably, while this transformation could not be achieved under Pd(0/II) catalysis and was moderately efficient at 2 mol% catalyst loading using MeDalPhos, high yields in cross coupling product were achieved at a loading as low as 0.3 mol% with ClKarPhos. Ultimately, this reactivity allowed us to develop a general divergent 2-step strategy to access various aryl sulfur derivatives. An additional computational and experimental study dedicated to determining the mechanism and the energetics of the transformation, highlighted the key role played by the silver salts in an off-cycle equilibrium.

Fundamentally, this study demonstrated the potential of (P^N) ligand for gold RedOx catalysis and the particular interest of the 2-NMe heteroaromatic fragment as the N-donor motif. We believe that structural and electronic variation on this platform would allow to easily and effectively tune the stability of the Au(III) intermediates and the barrier heights of the key OA and RE steps depending on their prevalence in a RedOx process. The study also highlights the value of predictive DFT calculations in the optimization of gold catalytic systems. The implementation of AI and machine learning in this process would most probably speed up the discovery of ligands allowing improved reactivity and specificity.

ACKOWLEDGEMENT This work was supported by the University of Ottawa and Natural Sciences and Engineering Research Council discovery grants (F. G. and M. V. B.). K. M. thanks the Faculty of Sciences and the department of Chemistry and Biomolecular Sciences at the University of Ottawa for providing an International Admission Scholarship, a Yu Scholarship and a Scaiano Scholarship. The authors are deeply appreciative of Prof. D. Pratt and Prof. T. Back for friendly scientific discussions on this project. The authors thank Dr. J. Ovens (University of Ottawa X-ray Core Facility) for his help with X-ray analyses, E. Caron for the large-scale synthesis of ligands **28** and **40**, and E. Gagosz-Faure for the design of the picture included in Figure 6-D.

REFERENCES

1. Recent reviews on homogeneous gold catalysis: (a) Lu, Z.; Li, T.; Mudshinge, S. R.; Xu, B.; Hammond, G. B. Optimization of Catalysts and Conditions in Gold(I) Catalysis—Counterion and Additive Effects. *Chem. Rev.* **2021**, *121*, 8452-8477. (b) Chintawar, C. C.; Yadav, A. K.; Kumar, A.; Sancheti, S. P.; Patil, N. T. Divergent Gold Catalysis: Unlocking Molecular Diversity through Catalyst Control. *Chem. Rev.* **2021**, *121*, 8478-8558. (c) Collado, A.; Nelson, D. J.; Nolan, S. P. Optimizing Catalyst and Reaction Conditions in Gold(I) Catalysis–Ligand Development. *Chem. Rev.* **2021**, *121*, 8559-8612. (d) Mato, M.; Franchino, A.; García-Morales, C.; Echavarren, A. M. Gold-Catalyzed Synthesis of Small Rings. Chem. Rev. 2021, 121, 8613-8684. (e) Campeau, D.; León Rayo, D. F.; Mansour, A.; Muratov, K.; Gagosz, F. Gold-Catalyzed Reactions of Specially Activated Alkynes, Allenes, and Alkenes. *Chem. Rev.* **2021**, *121*, 8756-8867. (f) Wang, T.; Hashmi, A. S. K. 1,2-Migrations onto Gold Carbene Centers. *Chem. Rev.* **2021**, *121*, 8948-8978. (g) Hendrich, C. M.; Sekine, K.; Koshikawa, T.; Tanaka, K.; Hashmi, A. S. K. Homogeneous and Heterogeneous Gold Catalysis for Materials Science. *Chem. Rev.* **2021**, *121*, 9113-9163.

2. de Meijere, A.; Diederich, F. Metal-Catalyzed Cross-Coupling Reactions; John Wiley & Sons, 2004.

3. For reviews and accounts on Au RedOx chemistry and cross-coupling reactions, see: (a) McCallum, T. Heart of gold: enabling ligands for oxidative addition of haloorganics in Au(i)/Au(iii) catalysed cross-coupling reactions. *Org. Biomol. Chem.* **2023**, *21*, 1629-1646. (b) Ambegave, S. B.; Patil, N. T. Gold-Catalyzed Cross-Coupling and 1,2-Difunctionalization -Reactions: A Personal Account. *Synlett* **2022**, *34*, 698-708. (c) Mishra, S.; Urvashi; Patil, N. T. Chiral Ligands for Au(I), Au(III), and Au(I)/Au(III) Redox Catalysis. *Isr. J. .Chem.* **2022**, e202200039. (d) Font, P.; Ribas, X. Fundamental Basis for Implementing Oxidant-Free Au(I)/Au(III) Catalysis. *Eur. J. Inorg. Chem.* **2021**, 2556-2569. (e) Zheng, Z.; Ma, X.; Cheng, X.; Zhao, K.; Gutman, K.; Li, T.; Zhang, L. Homogeneous Gold-Catalyzed Oxidation Reactions. *Chem. Rev.* **2021**, *121*, 8979-9038. (f) Witzel, S.; Hashmi, A. S. K.; Xie, J. Light in Gold Catalysis. *Chem. Rev.* **2021**, *121*, 8868-8925. (g) Huang, B.; Hu, M.; Toste, F. D. Homogeneous Gold Redox Chemistry: Organometallics, Catalysis, and Beyond. *Trends Chem.* **2020**, *2*, 707-720. (h) Banerjee, S.; Bhoyare, V. W.; Patil, N. T. Gold and hypervalent iodine(iii): liaisons over a decade for electrophilic functional group transfer reactions. *Chem. Commun.* **2020**, *56*, 2677-2690. (i) Meera, G.; Rohit, K. R.; Treesa, G. S. S.; Anilkumar, G. Advances and Prospects in Gold-Catalyzed C–H Activation. *Asian Journal of Organic Chemistry* **2020**, *9*, 144-161. (j) Nijamudheen, A.; Datta, A. Gold-Catalyzed Cross-Coupling Reactions: An Overview of Design Strategies, Mechanistic Studies, and Applications. *Chem. Eur. J.* **2020**, *26*, 1442-1487. (k) Fricke, C.; Reid, W. B.; Schoenebeck, F. A Review on Oxidative Gold-Catalyzed C-H Arylation of Arenes – Challenges and Opportunities. *Eur. J. Org. Chem.* **2020**, 7119-7130. (l) Zidan, M.; McCallum, T.; Thai-Savard, L.; Barriault, L. Photoredox meets gold Lewis acid catalysis in the alkylative semipinacol rearrangement: a photocatalyst with a dark side. *Org. Chem. Front.* **2017**, *4*, 2092-2096. (m) Hopkinson, M. N.; Tlahuext-Aca, A.; Glorius, F. Merging Visible Light Photoredox and Gold Catalysis. *Acc. Chem. Res.* **2016**, *49*, 2261-2272. (n) Zheng, Z.; Wang, Z.; Wang, Y.; Zhang, L. Au-Catalysed oxidative cyclisation. *Chem. Soc. Rev.* **2016**, *45*, 4448-445. (o) Miró, J.; del Pozo, C. Fluorine and Gold: A Fruitful Partnership. *Chem. Rev.* **2016**, *116*, 11924-11966.

4. Short selection of representative examples: with I(III) reagents, (a) Ball, L. T.; Lloyd-Jones, G. C.; Russell, C. A. Gold-catalyzed direct arylation. *Science* **2012**, *337*, 1644-1648. (c) Harper, M. J.; Emmett, E. J.; Bower, J. F.; Russell, C. A. Oxidative 1,2-Difunctionalization of Ethylene via Gold-Catalyzed Oxyarylation. *J. Am. Chem. Soc.* **2017**, *139*, 12386-12389. (b) Fricke, C.; Dahiya, A.; Reid, W. B.; Schoenebeck, F. Gold-Catalyzed C–H Functionalization with Aryl Germanes. *ACS Catal.* **2019**, *9*, 9231-9236. With selectfluor: (c) Zhang, G.; Peng, Y.; Cui, L.; Zhang, L. Gold-Catalyzed Homogeneous Oxidative Cross-Coupling Reactions. *Angew. Chem. Int. Ed.* **2009**, *48*, 3112-3115. (d) Brenzovich Jr., W. E.; Benitez, D.; Lackner, A. D.; Shunatona, H. P.; Tkatchouk, E.; Goddard III, W. A.; Toste, F. D. Gold-Catalyzed Intramolecular Aminoarylation of Alkenes: C-C Bond Formation through Bimolecular Reductive Elimination. *Angew. Chem. Int. Ed.* **2010**, *49*, 5519-5522. (e) Wang, W.; Jasinski, J.; Hammond, G. B.; Xu, B. Fluorine-Enabled Cationic Gold Catalysis: Functionalized Hydration of Alkynes. *Angew. Chem. Int. Ed.* **2010**, *49*, 7247-7252.

5. Short selection of representative examples: (a) Sahoo, B.; Hopkinson, M. N.; Glorius, F. Combining Gold and Photoredox Catalysis: Visible Light-Mediated Oxy- and Aminoarylation of Alkenes. *J. Am. Chem. Soc.* **2013**, *135*, 5505-5508. (b) Xie, J.; Sekine, K.; Witzel, S.; Krämer, P.; Rudolph, M.; Rominger, F.; Hashmi, A. S. K. Light-Induced Gold-Catalyzed Hiyama Arylation: A Coupling Access to Biarylboronates. *Angew. Chem. Int. Ed.* **2018**, *57*, 16648-16653. (c) Um, J.; Yun, H.; Shin, S. Cross-Coupling of Meyer–Schuster Intermediates under Dual Gold–Photoredox Catalysis. Org. Lett. 2016, 18, 484-487. (d) Xia, Z.; Khaled, O.; Mouriès-Mansuy, V.; Ollivier, C.; Fensterbank, L. Dual Photoredox/Gold Catalysis Arylative Cyclization of o-Alkynylphenols with Aryldiazonium Salts: A Flexible Synthesis of Benzofurans. *J. Org. Chem* **2016**, *81*, 7182-7190.

6. Two studies report the alternative use of a Buchwald ligand with reactions run at high temperature (140 °C). The use of such ligand implies higher energy barrier for the oxidative addition step, see: (a) Daley, R. A.; Morrenzin, A. S.; Neufeldt, S. R.; Topczewski, J. J. Gold Catalyzed Decarboxylative Cross-Coupling of Iodoarenes. *J. Am. Chem. Soc.* **2020**, *142*, 13210-13218. (b) Chen, G.; Xu, B. Hydrogen Bond Donor and Unbalanced Ion Pair Promoter-Assisted Gold-Catalyzed Carbon–Oxygen Cross-Coupling of (Hetero)aryl Iodides with Alcohols. *ACS Catal.* **2023**, *13*, 1823-1829.

7. Joost, M.; Zeineddine, A.; Estévez, L.; Mallet–Ladeira, S.; Miqueu, K.; Amgoune, A.; Bourissou, D. Facile Oxidative Addition of Aryl Iodides to Gold(I) by Ligand Design: Bending Turns on Reactivity. *J. Am. Chem. Soc.* **2014**, *136*, 14654-14657.

8. Zeineddine, A.; Estévez, L.; Mallet-Ladeira, S.; Miqueu, K.; Amgoune, A.; Bourissou, D. Rational development of catalytic Au(I)/Au(III) arylation involving mild oxidative addition of aryl halides. *Nat. Commun.* **2017**, *8*, 565.

9. (a) Rodriguez, J.; Zeineddine, A.; Sosa Carrizo, E. D.; Miqueu, K.; Saffon-Merceron, N.; Amgoune, A.; Bourissou, D. Catalytic Au(i)/Au(iii) arylation with the hemilabile MeDalphos ligand: unusual selectivity for electron-rich iodoarenes and efficient application to indoles. *Chem. Sci.* **2019**, *10*, 7183-7192. (b) Akram, M. O.; Das, A.; Chakrabarty, I.; Patil, N. T. Ligand-Enabled Gold-Catalyzed C(sp2)–N Cross-Coupling Reactions of Aryl Iodides with Amines. *Org. Lett.* **2019**, *21*, 8101-8105. (c) Zhang, S.; Wang, C.; Ye, X.; Shi, X. Intermolecular Alkene Difunctionalization via Gold-Catalyzed Oxyarylation. *Angew. Chem. Int. Ed.* **2020**, *59*, 20470-20474. (d) Rodriguez, J.; Adet, N.; Saffon-Merceron, N.; Bourissou, D. Au(i)/Au(iii)-Catalyzed C–N coupling. *Chem. Commun.* **2020**, *56*, 94-97. (e) Rigoulet, M.; Thillaye du Boullay, O.; Amgoune, A.; Bourissou, D. Gold(I)/Gold(III) Catalysis that Merges Oxidative Addition and π-Alkene Activation. *Angew. Chem. Int. Ed.* **2020**, *59*, 16625-16630. (f) Chintawar, C. C.; Yadav, A. K.; Patil, N. T. Gold-Catalyzed 1,2-Diarylation of Alkenes. *Angew. Chem. Int. Ed.* **2020**, *59*, 11808-11813. (g) Tathe, A. G.; Chintawar, C. C.; Bhoyare, V. W.; Patil, N. T. Ligand-enabled gold-catalyzed 1,2-heteroarylation of alkenes. *Chem. Commun.* **2020**, *56*, 9304-9307. (h) Rodriguez, J.; Tabey, A.; Mallet-Ladeira, S.; Bourissou, D. Oxidative additions of alkynyl/vinyl iodides to gold and gold-catalyzed vinylation reactions triggered by the MeDalphos ligand. *Chem. Sci.* **2021**, *12*, 7706-7712. (i) Tathe, A. G.; Urvashi; Yadav, A. K.; Chintawar, C. C.; Patil, N. T. Gold-Catalyzed 1,2-Aminoarylation of Alkenes with External Amines. *ACS Catal.* **2021**, *11*, 4576-4582. (j) Chintawar, C. C.; Bhoyare, V. W.; Mane, M. V.; Patil, N. T. Enantioselective Au(I)/Au(III) Redox Catalysis Enabled by Chiral (P,N)-Ligands. *J. Am. Chem. Soc.* **2022**, *144*, 7089-7095. (k) Rodriguez, J.; Vesseur, D.; Tabey, A.; Mallet-Ladeira, S.; Miqueu, K.; Bourissou, D. Au(I)/Au(III) Catalytic Allylation Involving π-Allyl Au(III) Complexes. *ACS Catal.* **2022**, *12*, 993-1003. (l) Tathe, A. G.; Patil, N. T. Ligand-Enabled Gold-Catalyzed C(sp2)–S Cross-Coupling Reactions. *Org. Lett.* **2022**, *24*, 4459-4463. (m) Ye, X.; Wang, C.; Zhang, S.; Tang, Q.; Wojtas, L.; Li, M.; Shi, X. Chiral Hemilabile P,N-Ligand-Assisted Gold Redox Catalysis for Enantioselective Alkene Aminoarylation. *Chem. Eur. J.* **2022**, *28*, e202201018. (n) Mudshinge, S. R.; Yang, Y.; Xu, B.; Hammond, G. B.; Lu, Z. Gold (I/III)-Catalyzed Trifluoromethylthiolation and Trifluoromethylselenolation of Organohalides. *Angew. Chem. Int. Ed.* **2022**, *61*, e202115687. (o) Bhoyare, V. W.; Sosa Carrizo, E. D.; Chintawar, C. C.; Gandon, V.; Patil, N. T. Gold-Catalyzed Heck Reaction. *J. Am. Chem. Soc.* **2023**, *145*, 8810-8816. (p) Das, A.; Patil, N. T. Ligand-Enabled Gold-Catalyzed C(sp2)–O Cross-Coupling Reactions. *ACS Catal.* **2023**, *13*, 3847-3853. (q) Bhoyare, V. W; Tathe, A. G.; Gandon, V; Patil, N. T. Gold-Catalyzed Interrupted Relay Heck Reaction. *ChemRxiv* **2023**, DOI: 10.26434/chemrxiv-2023-bzz0k. (r) Patil, N. T. ; Sancheti, S. P.; Singh, Y.; Mane, M. V. Gold-Catalyzed 1,2-

Dicarbofunctionalization of Alkynes. *ChemRxiv* **2023**, DOI: 10.26434/chemrxiv-2023-wd2l2.

10. (a) Harper, M. J.; Arthur, C. J.; Crosby, J.; Emmett, E. J.; Falconer, R. L.; Fensham-Smith, A. J.; Gates, P. J.; Leman, T.; McGrady, J. E.; Bower, J. F.; et al. Oxidative Addition, Transmetalation, and Reductive Elimination at a 2,2′-Bipyridyl-Ligated Gold Center. *J. Am. Chem. Soc.* **2018**, *140*, 4440-4445. (b) Cadge, J. A.; Sparkes, H. A.; Bower, J. F.; Russell, C. A. Oxidative Addition of Alkenyl and Alkynyl Iodides to a AuI Complex. *Angew. Chem. Int. Ed.* **2020**, *59*, 6617-6621. (c) Cadge, J. A.; Bower, J. F.; Russell, C. A. A Systematic Study of the Effects of Complex Structure on Aryl Iodide Oxidative Addition at Bipyridyl-Ligated Gold(I) Centers. *Angew. Chem. Int. Ed.* **2021**, *60*, 24976-24983.

11. (a) Gao, P.; Xu, J.; Zhou, T.; Liu, Y.; Bisz, E.; Dziuk, B.; Lalancette, R.; Szostak, R.; Zhang, D.; Szostak, M. L-Shaped Heterobidentate Imidazo[1,5-a]pyridin-3-ylidene (N,C)-Ligands for Oxidant-Free AuI/AuIII Catalysis. *Angew. Chem. Int. Ed.* **2023**, *62*, e202218427. (b) Scott, S. C.; Cadge, J. A.; Boden, G. K.; Bower, J. F.; Russell, C. A. A Hemilabile NHC-Gold Complex and its Application to the Redox Neutral 1,2-Oxyarylation of Feedstock Alkenes. *Angew. Chem. Int. Ed.* **2023**, *62*, e202301526.

12. (a) Font, P.; Valdés, H.; Guisado-Barrios, G.; Ribas, X. Hemilabile MIC^N ligands allow oxidant-free Au(i)/Au(iii) arylation-lactonization of γ-alkenoic acids. *Chem. Sci.* **2022**, *13*, 9351-9360. See also: (b) Navarro, M.; Tabey, A.; Szalóki, G.; Mallet-Ladeira, S.; Bourissou, D. Stable Au(III) Complexes Bearing Hemilabile P^N and C^N Ligands: Coordination of the Pendant Nitrogen upon Oxidation of Gold. *Organometallics* **2021**, *40*, 1571-1576.

13. Lundgren, R. J.; Sappong-Kumankumah, A.; Stradiotto, M. A Highly Versatile Catalyst System for the Cross-Coupling of Aryl Chlorides and Amines. *Chem. Eur. J.* **2010**, *16*, 1983-1991.

14. Genoux, A.; Biedrzycki, M.; Merino, E.; Rivera-Chao, E.; Linden, A.; Nevado, C. Synthesis and Characterization of Bidentate (P^N)Gold(III) Fluoride Complexes: Reactivity Platforms for Reductive Elimination Studies. *Angew. Chem. Int. Ed.* **2021**, *60*, 4164-4168.

15. For intramolecular stabilization of Au(III) (intermediate) complexes by a pyridine N-donor, see: (a) Serra, J.; Whiteoak, C. J.; Acuña-Parés, F.; Font, M.; Luis, J. M.; Lloret-Fillol, J.; Ribas, X. Oxidant-Free Au(I)-Catalyzed Halide Exchange and Csp2–O Bond Forming Reactions. *J. Am. Chem. Soc.* **2015**, *137*, 13389-13397. (a) Serra, J.; Parella, T.; Ribas, X. Au(iii)-aryl intermediates in oxidant-free C–N and C–O cross-coupling catalysis. *Chem. Sci.* **2017**, *8*, 946-952.

16. Gopalakrishnan, J. Aminophosphines: their chemistry and role as ligands and synthons. *Appl. Organomet. Chem.* **2009**, *23*, 291-318.

17. MeDalPhos can generally be purchased for ≈US$200/g.

18. Reiersølmoen, A. C.; Battaglia, S.; Orthaber, A.; Lindh, R.; Erdélyi, M.; Fiksdahl, A. P,N-Chelated Gold(III) Complexes: Structure and Reactivity. *Inorg. Chem.* **2021**, *60*, 2847-2855.

19. N-Me pyridine (P^N) ligands have been rarely employed in metal-mediated catalysis. See : (a) Yang, Y.; Gurnham, J.; Liu, B.; Duchateau, R.; Gambarotta, S.; Korobkov, I. Selective Ethylene Oligomerization with Chromium Complexes Bearing Pyridine–Phosphine Ligands: Influence of Ligand Structure on Catalytic Behavior. *Organometallics* **2014**, *33*, 5749-5757. (b) Blank, B.; Madalska, M.; Kempe, R. An Efficient Method for the Selective Iridium-Catalyzed Monoalkylation of (Hetero)aromatic Amines with Primary Alcohols. *Adv. Synth. Catal.* **2008**, *350*, 749-758. (c) Schareina, T.; Kempe, R. Combinatorial Libraries with P-Functionalized Aminopyridines: Ligands for the Preparation of Efficient C(Aryl)−Cl Activation Catalysts. *Angew. Chem. Int. Ed.* **2002**, *41*, 1521-1523.

20. See Supporting Information for details.

21. PAd_2 group cannot be ntroduced following this route.

22. When the SbF_6- counteranion was used, degradation was observed in situ.

23. For comparison, d(^{31}P) (MeDalPhos)Au(III)$Cl_2(PF_6)$= 109.8 ppm.

24. Dorta, R.; Stevens, E. D.; Scott, N. M.; Costabile, C.; Cavallo, L.; Hoff, C. D.; Nolan, S. P. Steric and Electronic Properties of N-Heterocyclic Carbenes (NHC): A Detailed Study on Their Interaction with Ni(CO)4. *J. Am. Chem. Soc.* **2005**, *127*, 2485-2495.

25. Caluclation perfoemd using the Xray crystal structure $\mathbf{29}_H$ and the SambVca 2.1 software available online at: https://www.molnac.unisa.it/OMtools/sambvca2.1/index.html.

26. Rigoulet, M.; Miqueu, K.; Bourissou, D. Mechanistic Insights about the Ligand-Enabled Oxy-arylation/vinylation of Alkenes via Au(I)/Au(III) Catalysis. *Chem. Eur. J.* **2022**, *28*, e202202110.

27. (a) Navarro, M.; Toledo, A.; Joost, M.; Amgoune, A.; Mallet-Ladeira, S.; Bourissou, D. π Complexes of P^P and P^N chelated gold(i). *Chem. Commun.* **2019**, *55*, 7974-7977. (b) Navarro, M.; Toledo, A.; Mallet-Ladeira, S.; Sosa Carrizo, E. D.; Miqueu, K.; Bourissou, D. Versatility and adaptative behaviour of the P^N chelating ligand MeDalphos within gold(i) π complexes. *Chem. Sci.* **2020**, *11*, 2750-2758.

28. (a) Neese, F. The ORCA program system. *WIREs Comput. Mol. Sci.* **2012**, *2*, 73-78. (b) Neese, F. Software update: the ORCA program system, version 4.0. *WIREs Comput. Mol. Sci.* **2018**, *8*, e1327.

29. (a) Bursch, M.; Mewes, J.-M.; Hansen, A.; Grimme, S. Best-Practice DFT Protocols for Basic Molecular Computational Chemistry. *Angew. Chem. Int. Ed.* **2022**, *61*, e202205735. (b) Grimme, S.; Hansen, A.; Ehlert, S.; Mewes, J.-M. r^{2}SCAN-3c: A "Swiss army knife" composite electronic-structure method. *J. Chem. Phys.* **2021**, *154*, 064103. (c) Dohm, S.; Hansen, A.; Steinmetz, M.; Grimme, S.; Checinski, M. P. Comprehensive Thermochemical Benchmark Set of Realistic Closed-Shell Metal Organic Reactions. *J. Chem. Theory Comput.* **2018**, *14*, 2596-2608.

30. This assumption was made by comparing the pKa of 4-CF_3pyridine (2.8) and pyrazine (0.6).

31. Other EWGs could be considered. The Cl atom was retained for its ease of introduction using the 2-NHMe-pyrazine intermediate leading to KarPhos as substrate (see Figure 5).

32. Kung, K. K.-Y.; Ko, H.-M.; Cui, J.-F.; Chong, H.-C.; Leung, Y.-C.; Wong, M.-K. Cyclometalated gold(iii) complexes for chemoselective cysteine modification via ligand controlled C–S bond-forming reductive elimination. *Chem. Commun.* **2014**, *50*, 11899-11902.

33. (a) Messina, M. S.; Stauber, J. M.; Waddington, M. A.; Rheingold, A. L.; Maynard, H. D.; Spokoyny, A. M. Organometallic Gold(III) Reagents for Cysteine Arylation. *J. Am. Chem. Soc.* **2018**, *140*, 7065-7069. (b) Stauber, J. M.; Rheingold, A. L.; Spokoyny, A. M. Gold(III) Aryl Complexes as Reagents for Constructing Hybrid Peptide-Based Assemblies via Cysteine S-Arylation. *Inorg. Chem.* **2021**, *60*, 5054-5062. (c) McDaniel, J. W.; Stauber, J. M.; Doud, E. A.; Spokoyny, A. M.; Murphy, J. M. An Organometallic Gold(III) Reagent for 18F Labeling of Unprotected Peptides and Sugars in Aqueous Media. *Org. Lett.* **2022**, *24*, 5132-5136.

34. Currie, L.; Rocchigiani, L.; Hughes, D. L.; Bochmann, M. Carbon–sulfur bond formation by reductive elimination of gold(iii) thiolates. *Dalton Transactions* **2018**, *47*, 6333-6343.

35. (a) Peng, H.; Cai, R.; Xu, C.; Chen, H.; Shi, X. Nucleophile promoted gold redox catalysis with diazonium salts: C–Br, C–S and C–P bond formation through catalytic Sandmeyer coupling. *Chem. Sci.* **2016**, *7*, 6190-6196. See also: (b) Caballero-Muñoz, A.; Rosas-Ortega, M.; Díaz-Salazar, H.; Porcel, S. C−S Cross-Coupling of Aryldiazonium Salts with Thiols Mediated by Gold. *Eur. J. Org. Chem.* **2023**, e202300203.

36. Kepp, K. P. A Quantitative Scale of Oxophilicity and Thiophilicity. *Inorg. Chem.* **2016**, *55*, 9461-9470.

37. Beletskaya, I. P.; Ananikov, V. P. Transition-Metal-Catalyzed C–S, C–Se, and C–Te Bond Formations via Cross-Coupling and Atom-Economic Addition Reactions. Achievements and Challenges. *Chem. Rev.* **2022**, *122*, 16110-16293.

38. *S*-Arylthiosulfonates are classicaly produced by oxidation using either aryl thiols, disulfides, sulfinates or sulfonyl derivatives as the substrates.

39. For two recent methods to install a STs group by umpolung onto a nucleophilic aromatic group, see: (a) Kanemoto, K.; Furuhashi, K.; Morita, Y.; Komatsu, T.; Fukuzawa, S.-i. Acid-Mediated Sulfonylthiolation of Arenes via Selective Activation of SS-Morpholino Dithiosulfonate. *Org. Lett.* **2021**, *23*, 1582-1587. (b) Jiang, Y.-F.; Zhu, W.-C.; Liu, X.-Y.; Tian, S.-Y.; Han, J.-H.; Rao, W.; Shen, S.-S.; Sheng, D.; Wang, S.-Y. Synthesis of 1,3-Dibenzenesulfonylpolysulfane (DBSPS) and Its Application in the Preparation of Aryl Thiosulfonates from Boronic Acids. *Org. Lett.* **2023**, *25*, 1776-1781.

40. Reeves, J. T.; Camara, K.; Han, Z. S.; Xu, Y.; Lee, H.; Busacca, C. A.; Senanayake, C. H. The Reaction of Grignard Reagents with Bunte Salts: A Thiol-Free Synthesis of Sulfides. *Org. Lett.* **2014**, *16*, 1196-1199.

41. The (MeDalPhos)Au-I complex was calculated to be slightly more stable than $\mathbf{45}_{STs}$ (ΔG= -1.3 kcal.mol^{-1}).

42. Chen, X.-Y.; Pu, M.; Cheng, H.-G.; Sperger, T.; Schoenebeck, F. Arylation of Axially Chiral Phosphorothioate Salts by Dinuclear PdI Catalysis. *Angew. Chem. Int. Ed.* **2019**, *58*, 11395-11399.

43. A PhSTs to IPh ligand exchange mediated by $AgSbF_6$ was calculated to be slightly more favorable (ΔG= +3.8 kcal.mol^{-1}).

44. Römbke, P.; Schier, A.; Wiesbrock, F.; Schmidbaur, H. Gold(I) thiosulfonate complexes. *Inorg. Chim. Acta* **2003**, *347*, 123-128.

45. At the beginning of the reaction, the ≈ 0.2 equiv. of Ag+ salt not complexed to TsS^- would most probably be in solution as κ-IAr-Ag(I) complexes. When the reaction progresses, □-S coordination to the ArSTs might become prevalent. "free" Ag+ salt refers to Ag+ not being consumed (to produce AgI) and present as complexes with a lower binding affinity ligand (ArI, ArSTs) than TsS^-.

46. The reaction was perfomed with MeDalPhos as the ligand due to the instability of the corresponding Au(III) complex when AuClKarPhos is employed.

47. A fast equlibrium should also be in play between the (P^N)Au(I)-I by-product of the reaction and the corrresponding (P^N)Au(I)-STs is used as the ligand.

48. For ArI with EWG, the electronic density on the iodine would be reduced and hence its Lewis basicity. A weaker binding to the Au(I) center should be expected.

49. The $\Delta G^{\neq}$ value for the oxidative addition step should also be affected by the presence of substituents on ArI. Preliminary results from DFT calculations show that these values differ by less than 2 $kcal.mol^{-1}$ when comparing the effect of a *para*-OMe versus *para*-CF_3 substituent.